Proceeding of the IEEE
International Conference on Robotics and Biomimetics
Dali, China, December 2019

# MC-Inverse: An Analytical Method for Consistent Motion of Anthropomorphic Dual-arm Robot*

Junyu Zou
*Institute of Robotics and Intelligent Systems*
*Wuhan University of Science and Technology*
*Wuhan, China*
zjy_yxys@163.com

Huasong Min†
*Institute of Robotics and Intelligent Systems*
*Wuhan University of Science and Technology*
*Wuhan, China*
mhuasong@wust.edu.cn

Hongcheng Xu
*Institute of Robotics and Intelligent Systems*
*Wuhan University of Science and Technology*
*Wuhan, China*
xuhcheng@gmail.com

***Abstract* - In order to keep the consistent of the dual-arm motion, an inverse kinematics method is proposed, which is called MC-inverse (Motion Consistency Inverse). Using the arm angle as an additional parameter to control the dual-arm in joint space, it can generate same arm angles when the anthropomorphic dual-arm robot repeats movement from similar initial position to the same target, and not only complete the human-like task, but also the motion is predictable and controllable. In this paper, we designed a dual-arm robot-HR2 as experimental platform to verify the proposed method, select the joint angles and arm angles as the evaluation values, to compare our method with Track-IK and ikfast methods. The comparison results show that our method can keep the consistent of motion better.**

***Index Terms* - *Anthropomorphic dual-arm robot, inverse kinematics, arm angle, Human-like manipulation, motion consistency.***

## I. INTRODUCTION

With the continuous expansion of the scope of application of robots, various new operational tasks and working environments have put forward higher requirements for the operation ability of robots. The dual-arm robot has the advantages of strong load capacity, high work efficiency and large working space[1, 2]. The anthropomorphic dual-arm robot has a structure similar to that of a human arm, and has flexible operation capability, which is relatively easy to be accepted by humans. It is an important development direction on the dual-arm robot and is also the main research on the human-like manipulation today[3]. At present, there are already many anthropomorphic dual-arm robots on the market, such as DLR Justin, NASA Robonaut2, Kawasaki Motoman and so on. Their common features are to adapt to the uncertainty of the working environment and the flexibility of the task.

In order to ensure the anthropomorphic dual-arm robot safely and accurately complete task, the robot must know the change of joint angle, and have the ability to adapt to different task, so that human can predict the state of the robot and improve the safety of human-robot interaction. The inverse kinematics method of the robot should ensure that the joint trajectory can be smoothly and the motion can be predicted when the arm move to the target. In view of the above problems, some solutions have been proposed.

*Inverse kinematics methods of the anthropomorphic arm*—The inverse kinematics problem of a manipulator is to map the position and rotation of the end effector in Cartesian Space to the joint space by coordinate transformation and calculate all the joint angles that can reach the given pose in the Joint Space[4]. The inverse kinematics method mainly includes numerical methods and analytical methods. The numerical methods are suitable for manipulators with arbitrary structure, and keep the optimization ability of redundant manipulators [5,6]. However, it is slow to calculate and cannot limit the motion of the arm, the joint angles is unpredictable. The most common method in numerical methods is to create a Jacobian matrix of the manipulator, mapping directly from the operational space to the joint space[7, 11]. They are iterated by Newton method or other methods until the solution "sufficiently close" to the target pose of the end-effector. At present, the more commonly used numerical solution is KDL (Orocos Kinematics and Dynamics Library). And Beeson et al. have improved and optimized the problems of KDL (stuck at local minimum, easy to solve under joint constraints, etc). The Trac-IK solver is proposed, which improves the speed of solution and the success rate of solution[8]. For the anthropomorphic arm, it has 7-DOF, there is a redundant joint. So the core idea of the analytical solution is to eliminate redundancy[9,12]. Dianov et al. proposed the ikfast solver[10], which first fixes a joint to solve other joints. Since the method requires prior knowledge of the arm structure, the solver is constructed according to the structure, so the versatility and optimizability are poor.

If we expected to predict the anthropomorphic arm motion, then in the process of planning the trajectory, not only the end-effector is always on the desired trajectory, but also the arm motion is always consistent with our expectations (such as human-like motion). But for the anthropomorphic arm, there is a redundant-DOF, so it is countless inverse kinematics solutions. Even given the trajectory of the end-effector, the motion of the arm (joint angle) is often unpredictable. In order to control the arm motion of the

*This work is supported by National Key R&D Program of China (Project No. 2017YFB1300400), National Natural Science Foundation of China (Project No. 6 1673304) and Wuhan Science and Technology Planning Project (Project No.2018010401011275).
†Huasong Min is the corresponding author.



978-1-7281-6321-5/19//$31.00 ©2019 IEEE

anthropomorphic dual-arm robot, Shin and Kim use a demonstration learning method in the dual-arm operation to generate anthropomorphic motion using the acquired human motion data[13]. Xu et al. proposed the kinematics method based on the physiological structure corresponding to the anthropomorphic arm and determined that the entire arm was mapped back to the joint space for execution. This method not only retains the optimization ability of the anthropomorphic arm, but also controls the arm motion[14].

However, there is still an important problem at present, which is the repeatability of task. Most of the people research on dual-arm robot is limited to one target or one task, that is, from an initial waypoint move to a target waypoint. Due to the unpredictability of the anthropomorphic arm, even if the task can be completed on one target, it is difficult to ensure that the arm motion is consistent with our expectations when the arm move to the same target. An example is shown in Fig. 1, we let the robot draw a complete circle in Cartesian space. Fig. 1(a) shows the arm initial state. After the drawing, the end-effector pose is exactly the same as the initial one, but the joint angles are different from the initial state (Fig. 1 (b)). Based on this type of problem, this paper presents the problem of *Motion Consistency*: ***Whether the arm motion of the anthropomorphic dual-arm robot is exactly the same when repeatedly performing the same task or moving along the same trajectory***.

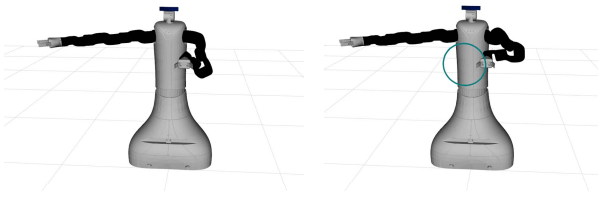

**(a) The initial state** **(b) Drawing the circle**

Fig. 1 Inconsistency in motion of anthropomorphic manipulator

The anthropomorphic arm motion may be completely different even if they accomplish the same task. But this kind of problem does not happen every time, so it is hard to find the problem and a law that can be followed. In fact, when the robot performs multiple tasks and repetitive work, the arm motion may change obviously on the same target, which may eventually lead to the failure of the task.

In order to solve this problem, this paper mainly does the following two tasks. First of all, we propose an MC-Inverse (Motion Consistency Inverse) method. This method can make the robot generate human-like motion, and can predict the next motion to constrain and control the arm, so that the arm can ensure the consistency of the motion when move to the same target. In addition, in order to fully utilize the advantages of the anthropomorphic dual-arm robot, a dual-arm coordinated operation method is proposed and arm control is performed in the process.

The rest of the paper is organized as follows. Following this introduction, Section II introduces the experimental platform of this paper. Section III analyzes the inverse kinematics method of the most commonly used anthropomorphic arm at present, and introduces the method of this paper. Section IV introduces the realization of the two-arm coordinated operation method Section V gives the experimental results of the consistency between the inverse kinematics method and the commonly used inverse kinematics method on the anthropomorphic arm. Finally, the conclusions and future directions are offered in Section VI.

## II. Experimental Platform Introduction

The HR2 dual-arm robot designed in this paper is shown in Fig. 2. The robot arm adopts the design idea of the anthropomorphic arm. The anthropomorphic arm has a Spherical-Revolute-Spherical (S-R-S) structure[15]. Usually, it is consist of 7 revolute joints. The axes of the first three joints intersect at one point and form a spherical joint equivalently, thus realizing the physiological shoulder joint; the fourth joint corresponds to the elbow joint; and the axes of the last three joints also intersect at one point, forming a spherical joint to realize the wrist joint. As shown in Fig. 3.

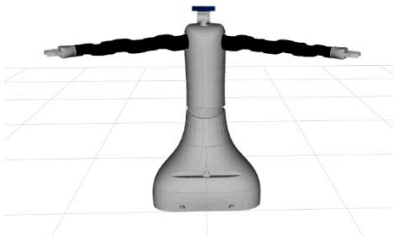

Fig. 2 HR2 robot model

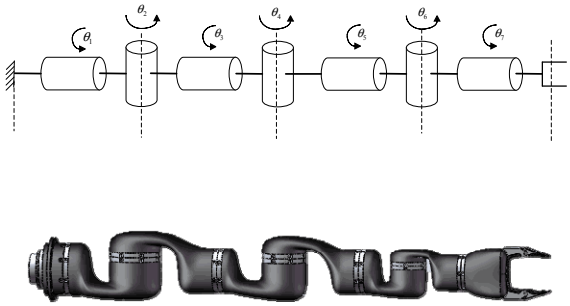

Fig. 3 Anthropomorphic arm structure and HR2 robot arm designed in this structure

## III. Comparative Analysis of Inverse Kinematics Methods

### A. Inverse kinematics method

In order to generate a feasible motion trajectory, the anthropomorphic arm initial state is usually known, and then set the end-effector pose. Finally, a feasible path is planned by using trajectory planning method (such as OMPL [16]), and the waypoints on the path are solved by inverse kinematics (IK) to obtain the trajectory. The joint angle of the anthropomorphic arm corresponding to each waypoint. There

are many inverse kinematics methods for anthropomorphic arm. However, these methods not always achieve the desired results. For example, we expect arm motion to be human-like, predictable and controllable. However, the commonly used inverse kinematics methods cannot achieve these results. This paper lists two of the most commonly used inverse solutions, which are compared with our method for the motion consistency.

a) Trac-IK

The first chapter mentions that Beeson et al. has proposed the Trac-IK solver [8], which is the most advanced numerical solution at present, and is one of the main methods of comparison in this paper. Trac-IK still keep the optimization ability of the anthropomorphic arm. However, this method is only related to the end-effector pose of the arm, and not related to arm motion. When generating a series of solutions, especially in the same target, the motion of the arm is unpredictable, so there is no guarantee that a consistent and feasible motion will be obtained. Worse, this method may be Instantaneous jumps occur in the joint space and may cause damage to the robot due to self-collision.

b) ikfast

The main analytical method of this paper is ikfast [10], ikfast can solve the kinematic equation of any complex kinematic chain by sacrificing some generality.

For the anthropomorphic arm, ikfast selects a joint that is Least important, and assumes that it was set before running IK, called the free joint, and the joint that IK solves is called the active joint. During the solution process, the range of the free joint is discretized and all values are tested until a solution that satisfies the joint limit, collision, and planning constraints is found. The dispersion of this free space depends on the importance of the joint, so that the analytical solution of the anthropomorphic arm can be obtained. The disadvantage of ikfast is that poor universality, and the structure of the arm must be known in advance and the optimization ability is lost.

### *B. Motion Consistency Inverse*

As mentioned above, the arm of the HR2 robot is an anthropomorphic arm which has a self-motion that rotates around the shoulder-wrist axis, which does not affect the pose of the end-effector. Based on this, Kreutz-Delgado et al. defined the angle between the plane defined by the shoulder, elbow and wrist center and the vertical plane of the shoulder-wrist line as the *arm angle*[17]. This paper extends this idea to the anthropomorphic dual-arm robot, using the arm angle to describe the redundant-DOF, and controlling the arm motion. At the same time, the MC-Inverse method of this paper is proposed, which can keep the anthropomorphic arm motion consistency when move to the same target. We decompose the inverse kinematic into three sub-problems. One of the characteristics of the sub-problems mentioned here is that they have clear geometric meaning and numerical stability. The arm angle $\psi$ is used to describe the motion of the anthropomorphic arm because it is closely related to the self-motion of the anthropomorphic arm rotating around the shoulder-wrist line.

The origin of the shoulder coordinate system is the point where the first three joint axes intersect. The origin of the elbow coordinate system is the center of the fourth joint. The origin of the wrist coordinate system is the point where the last three joint axes intersect. And is represented by S, E, and W, respectively, as shown in Fig. 4.

In Fig. 4, the arm angle is the angle between the arm plane and the reference plane. The arm plane defined by the center of the shoulder (S), the elbow (E), and the wrist (W), the vertical plane of the shoulder-wrist line. Where O is the base coordinate system of the arm, which is set to the x-axis pointing forward and the z-axis vertically upward. T is the end-effector coordinate system of the robot arm, and L1, L2, L3, and L4 are known quantities, which are determined by the structure of the arm itself.

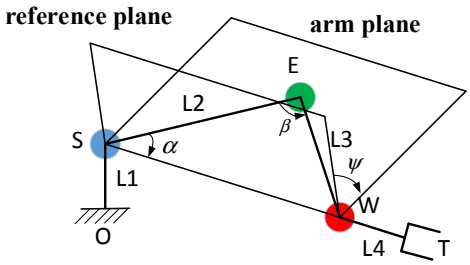


Fig. 4 Arm angle definition and geometric relationship

The reference plane chosen in this paper is defined by the vector $\overrightarrow{SW}$ and the vertical vector $\vec{V} = [0 \quad 0 \quad 1]^T$, setting the arm angle when the elbow joint is below, so the arm angle is defined as (1):

$$\psi = a\tan 2(-(\overrightarrow{n_{ref}} \times \overrightarrow{n_{arm}}) \cdot \frac{\overrightarrow{SW}}{\|SW\|}, \overrightarrow{n_{ref}} \cdot \overrightarrow{n_{arm}}) \tag{1}$$

In Equation (1), $\overrightarrow{n_{ref}}$ represents the normal vector of the reference plane, $\overrightarrow{n_{arm}}$ represents the normal vector of the arm plane, and the range of the arm angle is $(-\pi, \pi)$.

Given the end-effector position $P(P = [px \quad py \quad pz])$ and rotation $R$, and the arm angle of the anthropomorphic arm. According to the characteristics of the SRS structure of the arm, we can decompose the inverse problem of the arm into three sub-problems, namely the joint angle of the rotating joint (elbow joint) and the joint angle of the two spherical joints (shoulder joint, wrist joint). In this way, we can solve all the joint angles of the anthropomorphic arm.

a) sub-problem 1: elbow joint angle $\theta_4$

Vector $\overrightarrow{SW}$ can be obtained from the geometric relations in the Fig. 4 :

$$\overrightarrow{SW} = \overrightarrow{OT} - \overrightarrow{OS} - \overrightarrow{WT} \tag{2}$$

In Equation (2), $\overrightarrow{OT} = [px \quad py \quad pz]^T$, $\overrightarrow{OS} = [0 \quad 0 \quad L_1]^T$, $\overrightarrow{WT} = R[0 \quad 0 \quad L_4]^T$ are known quantities.

From the cosine theorem, we can directly find the $\beta$ in Fig. 4:

$$\beta = a\cos\left(\frac{L_2^2 + L_3^2 - \left\|\overrightarrow{SW}\right\|^2}{2L_2L_3}\right) \tag{3}$$

Because $\theta_4$ is a joint angle, it may be positive or negative, so $\theta_4$ as shown in equation (4):

$$\theta_4 = \begin{cases} \pi - \beta & (\theta_4 \geq 0) \\ \beta - \pi & (\theta_4 < 0) \end{cases} \tag{4}$$

b) sub-problem 2: shoulder joint angle $\theta_1, \theta_2, \theta_3$

Since the position $P_E$ and rotation $R_E$ of the center of the elbow joint are determined by the shoulder joint, it is only necessary to calculate the transformation matrix of the center of the elbow joint relative to the base, that is $P_E$ and $R_E$. The three joint angles of the shoulder joint can be calculated. From the geometric relationship in the Fig. 4 can get equation (5).

$$\begin{bmatrix} P_E \\ 1 \end{bmatrix} = e^{\hat{\xi}_{SW}\psi} e^{\hat{\xi}_{ref}\alpha} \begin{bmatrix} L_2 \dfrac{\overrightarrow{SW}}{\left\|\overrightarrow{SW}\right\|} \\ 1 \end{bmatrix} \tag{5}$$

In Equation (5), $\xi_{SW} = \begin{bmatrix} 0 & -\dfrac{\overrightarrow{SW}}{\left\|\overrightarrow{SW}\right\|} \end{bmatrix}^T$ is defined as the screw of the shoulder and wrist line, $\xi_{ref} = \begin{bmatrix} 0 & -\dfrac{\overrightarrow{n_{ref}}}{\left\|\overrightarrow{n_{ref}}\right\|} \end{bmatrix}^T$ is defined as the screw of rotation about the reference plane normal vector.

The direction vector of the elbow joint as shown in equation (6):

$$\omega_E = \frac{\overrightarrow{SE} \times \overrightarrow{SW}}{\left\|\overrightarrow{SE} \times \overrightarrow{SW}\right\|} \tag{6}$$

The rotation matrix of the elbow joint relative to the base coordinate system can be calculated from the direction vector and $\overrightarrow{SE}$. The formula is shown as (7):

$${}^O_E R = \begin{bmatrix} \dfrac{\overrightarrow{SE}}{\left\|\overrightarrow{SE}\right\|} & \omega_E \times \dfrac{\overrightarrow{SE}}{\left\|\overrightarrow{SE}\right\|} & \omega_E \end{bmatrix} \tag{7}$$

Then the joint angle of the shoulder joint is calculated. As mentioned above, the base of the shoulder joint is the base of the arm and the end is the center of elbow joint. Due to the particularity of the equivalent spherical joint, the three joint angles constitute the ZYZ euler angle about the base coordinate system, so assume that the rotation matrix obtained as shown in equation (8):

$${}^O_E R = \begin{bmatrix} r_{11} & r_{12} & r_{13} \\ r_{21} & r_{22} & r_{23} \\ r_{31} & r_{32} & r_{33} \end{bmatrix} \tag{8}$$

The three joint angles of the shoulder joint $(\theta_1, \theta_2, \theta_3)$ can be calculated directly. For $\theta_2 \in (0, \pi)$, there are:

$$\begin{aligned} \theta_1 &= a\tan 2(r_{23}, r_{13}) \\ \theta_2 &= a\tan 2(\sqrt{(r_{13})^2 + (r_{23})^2}, r_{33}) \\ \theta_3 &= a\tan 2(r_{32}, -r_{31}) \end{aligned} \tag{9}$$

For $\theta_2 \in (0, \pi)$, there are:

$$\begin{aligned} \theta_1 &= a\tan 2(-r_{23}, -r_{13}) \\ \theta_2 &= a\tan 2(-\sqrt{(r_{13})^2 + (r_{23})^2}, r_{33}) \\ \theta_3 &= a\tan 2(-r_{32}, r_{31}) \end{aligned} \tag{10}$$

c) sub-problem 3: wrist joint angle $\theta_5, \theta_6, \theta_7$

Similar to sub-problem 2, the wrist joint angle can be calculated from the rotation matrix of the center of elbow joint to end-effector. The base coordinate system of the wrist joint is the center of elbow joint, the end is the end-effector, and the rotation matrix is ${}^E_T R$. From equations (8), (9), and (10), the three joint angles of the wrist joint can be calculated.

Each of the above three sub-problems can calculate 2 sets of inverse solutions, so using this method, for a given set of end-effector pose and arm angle, a total of 8 sets of inverse solutions can be calculated. Then according to the existence of the solution, the invalid inverse solution is eliminated.

## IV. DUAL-ARM COORDINATED OPERATION METHOD

The anthropomorphic dual-arm robot not only need to be able to control the arm motion, but also need to have better coordination between the two arms in the execution of dual-arm operation. An example is shown in Fig. 5.

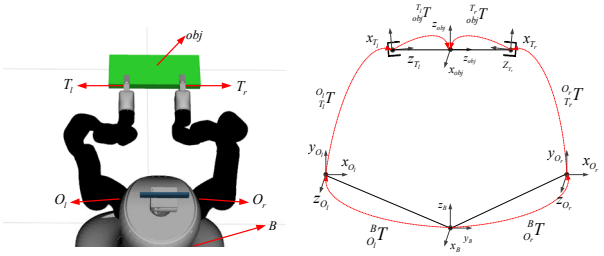


**(a) Dual-arm coordinated task** **(b) System coordinate transformation relationship**

Fig. 5 Dual-arm coordinated operation task system

If we hope the robot move the object from the initial position to the target position by dual-arm coordination, then we need to design a trajectory of Cartesian Space, and use the master-slave planning method to let slaver arm follow the master arm. We need to keep the object between the master arm and the slave arm during the movement. The dual-arm operation task requires that the end-effector and the object do not move relative to each other, and no relative movement occurs between the two arms.

As shown in Fig. 5(a), it is a dual-arm robot, it is necessary to establish a base coordinate system of the robot itself, called *Base_Link*, which is simply referred to as *B*. The base coordinate systems of the left arm and the right arm are $O_l$ and $O_r$. And the end are $T_l$ and $T_r$, and the left arm is the master arm and the right arm is the slave arm. The *obj* represents the coordinate system of the object being operated. In the centroid of the object, the coordinate transformation relationship is shown in Fig. 5(b).

According to the coordinate transformation relationship:

$$ {}^{B}_{O_l}T\,{}^{O_l}_{T_l}T\,{}^{T_l}_{obj}T = {}^{B}_{O_r}T\,{}^{O_r}_{T_r}T\,{}^{T_r}_{obj}T \tag{11} $$

In Equation (11), ${}^{B}_{O_l}T$ and ${}^{B}_{O_r}T$ are defined as the transformation matrix of the master and slaver arm coordinate systems relative to the base coordinate system. ${}^{T_l}_{obj}T$ and ${}^{T_r}_{obj}T$ are defined as the transformation matrix of the object relative to the end-effector of the master and slaver arm, all of which are constant matrices that are fixed during motion. ${}^{O_l}_{T_l}T$ and ${}^{O_r}_{T_r}T$ are defined as the transformation matrix of the end-effector relative to the arm base coordinate systems.

After planning the path of the dual-arm coordinated operation, it is also necessary to constrain the velocities and accelerations between the dual-arm. We use TOPP (time-optimal path parameterization) algorithm[18], input the position information (joint angle) of all waypoints in the dual-arm path, and calculate the velocities, accelerations and time information of all waypoints according to the principle of time optimization, so we can get a smooth trajectory in the Joint Space.

## V. Experiment

### A. MC-Inverse method test

We test the MC-Inverse inverse kinematics method on HR2 robot. Considering the motion human-like problem, we limit the range of the arm angle to $(-\pi, 0)$. Fig. 6 is a test example of the method, in which the position $P$ and rotation $R$ of the end-effector are: ( $P$:[0.147 –0.404 0.455] (m) $R$:[0.937 0.560 –0.377] (rad)) (relative to the arm base coordinate system, the rotation $R$ is represented by the xyz Euler angle), and the arm angle is set to 2.2(rad). Using our method to calculate the inverse solution, there are only 4 sets of inverse solutions after eliminating the invalid solution (Table I). Then control the arm to move to the calculated joint angle (Fig. 6). It can be seen that due to the existence of the arm angle parameter, the arm angle of the 4 sets of inverse solutions obtained by our method is completely identical. For each set of solutions, only the shoulder joints (blue dotted box in Fig. 6) and the wrist joints (red dotted box in Fig. 6) have different joint angles. Therefore, we can use the arm angle to control the motion of the arm.

TABLE I MC-Inverse method inverse solution test results

| Joint Angles ( rad ) | | Number of inverse solutions | | | |
|---|---|---|---|---|---|
| | | 1 | 2 | 3 | 4 |
| Shoulder Joint | $\theta_1$ | -1.84799 | -1.29361 | -1.84799 | 1.29361 |
| | $\theta_2$ | 0.21282 | -0.21282 | 0.21282 | -0.21282 |
| | $\theta_3$ | -2.08281 | 1.05878 | -2.08281 | 1.05878 |
| Elbow Joint | $\theta_4$ | -1.94261 | -1.94261 | -1.94261 | -1.94261 |
| Wrist Joint | $\theta_5$ | 0.54827 | 0.54827 | -2.59332 | -2.59332 |
| | $\theta_6$ | 1.29769 | 1.29769 | -1.29769 | -1.29769 |
| | $\theta_7$ | 1.38904 | 1.38904 | 1.75256 | 1.75256 |

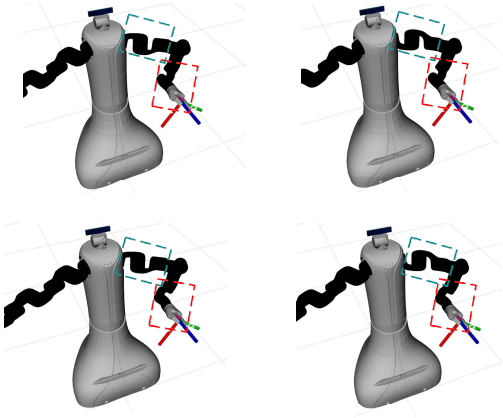

Fig. 6 MC-Inverse method inverse kinematics test results

### B. Motion Consistency Test (Line)

We take the consistency of motion as the evaluation index, compare the MC-Inverse and the commonly used inverse kinematics methods, and the experimental platform is HR2 robot. We let the left arm change the position and rotation in Cartesian space to draw a triangle repeatedly. The initial state of the arm is shown in Fig. 7.

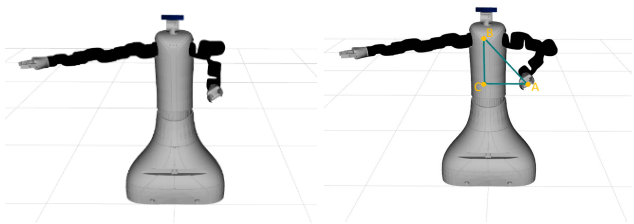

Fig. 7 Triangle repeated drawing experiments by robot changing position and rotation

The 3 vertices of the triangle are 3 points are:

$$A:\begin{matrix} P_a:[0.300 \quad 0.270 \quad 1.003](m) \\ R_a:[-1.572 \quad -0.975 \quad -1.570](rad) \end{matrix}$$

$$B:\begin{matrix} P_b:[0.300 \quad 0 \quad 1.303](m) \\ R_b:[-0.517 \quad -1.380 \quad 2.390](rad) \end{matrix}$$

$$C:\begin{matrix} P_c:[0.300 \quad 0 \quad 1.003](m) \\ R_c:[-1.573 \quad -1.435 \quad 1.581](rad) \end{matrix}$$

(The position and rotation of the 3 points A, B, C are relative to the robot base coordinate system)

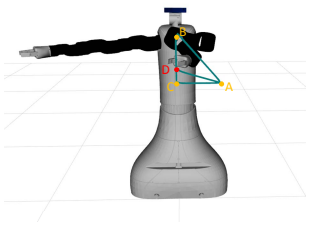


Fig. 8 Distortion arm and failed motion caused by inconsistency of motion in Trac-IK method

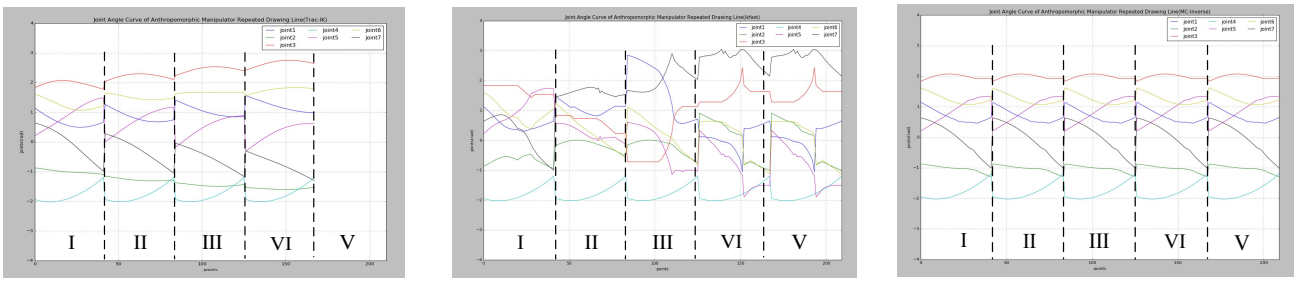


**(a) Trac-IK** **(b) ikfast** **(c) MC-Inverse**

Fig. 9 Curve of the joint angle of the arm when the triangle is repeated drawing by different inverse kinematics methods

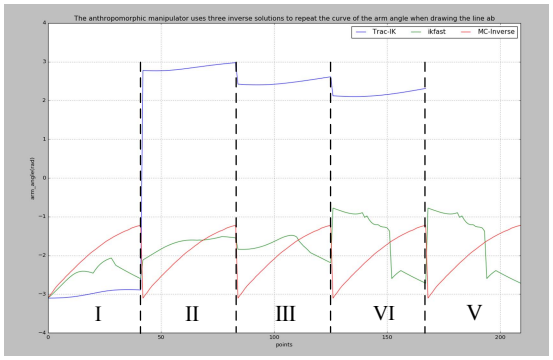


Fig. 10 Curve of the arm angle of the arm when the triangle is repeated drawing by different inverse kinematics methods

Fig. 9 (a), (b) show that the joint angle is different when it passes through the line AB with Trac-IK and ikfast methods, that is, the arm motion will change. This also verifies the inconsistency of the arm during repeated motion mentioned above. Our method can adjust and control the arm motion to ensure the consistency of the arm motion and the human-link movement each time passes through the AB (Fig. 9(c), The arm angle is adjusted and limited within $(-\pi,0)$ ).

Different inverse kinematics methods are used for HR2 rob ot to repeatedly draw the triangle 5 times. In the experiment, the Trac-IK method can't draw the desired complete triangle when the triangle is drawn for the fourth time. The arm moves to the point D in Fig. 8 and moves directly to point A. And the fifth is to stop directly. This is caused by the uncontrollable arm motion and easily enters the joint limit and causes the movement to fail.

We output the arm joint angle variation curve (Fig. 9) and the arm angle variation curve (Fig. 10) when drawing line AB each time the triangle is drawn. In order to clearly show the change range of the arm motion in motion, the abscissa (points) of the change curve in the graph are expressed as the waypoints (not the time) of the arm's trajectory. In Fig. 9 and Fig. 10, We use the Roman numerals I, II…V to indicate the changes of joint angle and arm angle when it passes through line AB for the first to fifth time. (The first plate indicates the first pass through the line AB, the second block indicates the second pass through the line AB, the other similar). Trac-IK has no data for the fifth time due to movement failure.

It can be seen from the comparison tasks of Fig. 9 and Fig. 10 that the Trac-IK fails to complete the task due to reaching the joint limit, and the arm motion changes when it is repeatedly executed. The ikfast completed the task, but the constraint of the free joint resulted in a large change in the arm motion and a discontinuous joint space. And the MC-Inverse can adjust the arm angle by changing the arm angle when the arm performs repeated motion.

### *C. Motion Consistency Test (Circle)*

In this paper, the HR2 robot repeatedly draws a circle to compare the motion consistency. We do not change the rotation of the end-effector at this time, only change the position to draw a circle. The initial state of the arm is shown in Fig. 11(a). The radius of the circle is set to 0.15m, the centre of the circle is $P:[0.293 \quad 0 \quad 1.05](m)$, and the position and rotation of the end-effector are:

$$P:[0.293 \quad 0.15 \quad 1.05](m)$$

$$R:[-1.571 \quad 1.571 \quad -1.571](rad)$$

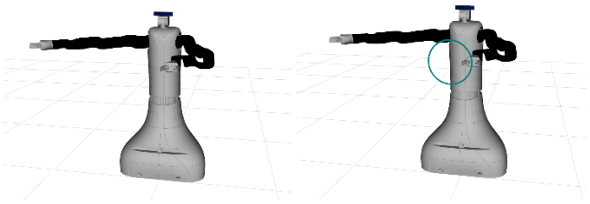

**(a) The initial state** **(b) Drawing the circle repeatly**

Fig. 11 Circle repeated drawing experiments by robot changing position

We also use different inverse kinematics methods to repeatly draw the circle 5 times (Fig. 11(b)), and output the joint angle curve (Fig. 12) and the arm angle curve (Fig. 13) of the robot arm each time the circle is drawn.

Similar to the repeated drawing of triangles, in Fig. 12 and Fig. 13, we use Roman numerals I, II...V to indicate the joint angle and arm angle change of the first to fifth time of the arm. Compared with the previous section, it can be seen that when Trac-IK and ikfast are used without changing the rotation, the smoothness and motion consistency of the arm in the joint space are greatly improved. But there didn't fully achieve the desired effect.

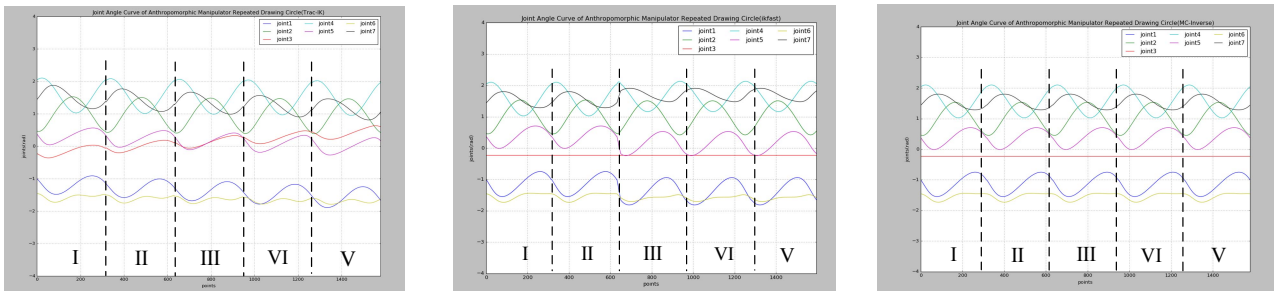


**(a) Trac-IK** **(b) ikfast** **(c) MC-Inverse**

Fig. 12 Curve of the joint angle of the arm when the circle is repeated drawing by different inverse kinematics methods

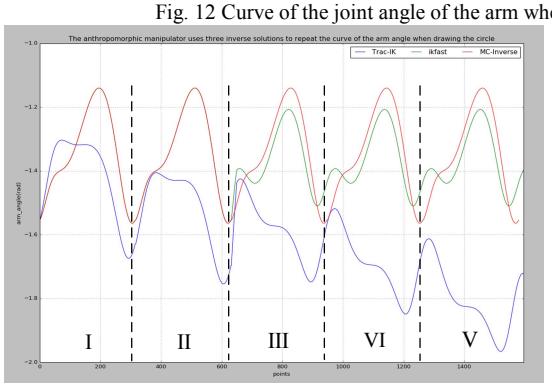


Fig. 13 Curve of the arm angle of the arm when the circle is repeated drawing by different inverse kinematics methods.

Fig. 12(a) shows the joint angle curve obtained by the Trac-IK, Fig. 12(b) shows the joint angle curve obtained by the ikfast, and Fig. 12(c) shows the joint angle obtained by the MC-Inverse. Comparing Fig. 12, Fig. 13 show that the Trac-IK method changes the joint angle every time the circle is drawn, resulting in inconsistent motion (such as joint angles 1, 3, 5, 7). The ikfast method in terms of motion consistency better than Trac-IK, but the arm angle changed when the third circle was drawn. The motion consistency could not be fully guaranteed. And our method can still effectively guarantee the motion consistency and achieve the desired effect.

### *D. Dual-arm coordinated operation and its consistency experiment*

For the dual-arm coordinated operation of the HR2 robot, this paper first tests the effect of our dual-arm coordinated operation method. We let the robot hold a cuboid. We first plan a path for the end-effector of the master arm, and according to formula (11) calculate the path from the end-effector of the slaver arm, and then calculate the inverse kinematics of the master arm and the slave arm respectively. Finally, use the smoothing of the joint space trajectory to obtain a complete dual-arm trajectory, and transport the cuboid to another position, such as Fig. 14 shows.

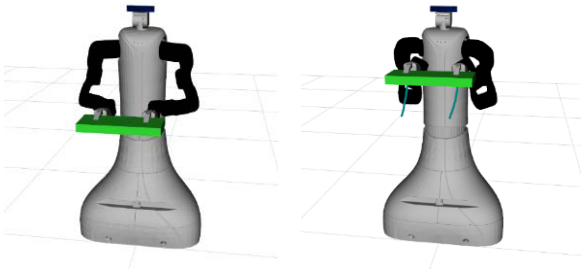

**(a) Initial position** **(b)Goal position**

Fig. 14 Example of dual-arm coordinating moving objects

This paper also tests the problem of motion consistency in the dual-arm coordinated operation. This time we directly set the initial state of the robot arm to be human-like, as shown in Fig. 15, indicating that the object is in the initial position. We let the robot hold the object up and down linear motion. In order to facilitate the observation of the dual-arm trajectory and motion, we hide the object. Fig. 16 shows the arm motion after using Track-IK, ikfast, and MC-Inverse.

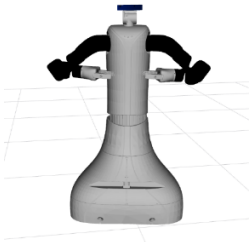

Fig. 15 Dual-arm state in the initial position of the object

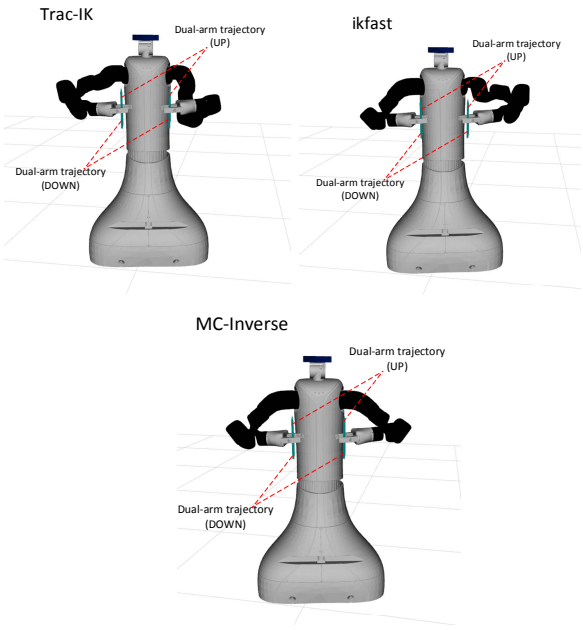


Fig. 16 Arm motion changes of two arms with different inverse kinematics methods when dual-arm coordinate in repetitive motion

It can be seen from Fig. 16 that during the coordinated operation of the two arms, the Trac-IK and ikfast inverse solution methods can accomplish the task, but the arm angle will change significantly. Because the ikfast inverse solution is an analytical method, it has a certain degree of constraint on the robot arm, so the arm motion variation is smaller than Trac-IK. With our method, the robot not only completes the task, but also ensures the consistency of the arm motion during the repeated motion.

## VI. Conclusion

In this paper, the motion controllability and consistency of the anthropomorphic dual-arm robot is studied, a novel method of inverse kinematics is proposed, which uses the arm angle to describe the redundancy degrees. It predicts and controls the motion of designed anthropomorphic dual-arm according to the value of the arm angle. Using the joint angle and the arm angle as the evaluation values, we compared the method of this paper with the commonly used inverse methods such as Trac-IK (numerical method) and ikfast (analytical method) of the anthropomorphic dual-arm robot, experiment scenes including single-arm and dual-arm motion. The comparison results show that our method can better guarantee the consistency of the arm when the robot performs the same task repeatedly. Therefore, our method can predict and control the motion of the anthropomorphic dual-arm robot, and ensure the motion consistency. It not only improves the ability of human-robot interaction, but also makes the task with repeatability.

Because the inconsistency problem of motion when the arm move to the same target does not occur every time, so we will explore under what kind of situation (or probability) the motion inconsistency will occur for further study.

## Acknowledgment

I would like show my deepest gratitude to the Dr. Zhou Haotian, who has provided me with valuable guidance in the writing of this thesis.

## References

[1] Y Wang, C Smith, Y Karayiannidis, et al. “Cooperative control of a serial-to-parallel structure using a virtual kinematic chain in a mobile dual-arm manipulation application,” Hamburg, Germany: *IEEE/RSJ International Conference on Intelligent Robots and Systems (IROS)*, vol. 12, pp. 2372-2379, December 2015.

[2] J Lemburg, et al, “AILA - design of an autonomous mobile dual-arm robot,” Shanghai, China: *IEEE International Conference on Robotics and Automation (ICRA)*. vol. 5, pp. 9-13. May 2011.

[3] F Zacharisa, C Schlette, et al, “Making planned paths look more human-like in humanoid robot manipulation planning,” Shanghai, China: *IEEE International Conference on Robotics and Automation (ICRA)*, vol. 5, pp. 1192-1198, May 2011.

[4] John J. Craig. *Introduction to Robotics: Mechanics and Control,* Introduction to Robotics Mechanics and Control, 1955.

[5] A Atawnih , D Papageorgiou, Z Doulgeri, “Kinematic control of redundant robots with guaranteed joint limit avoidance,” *Robotics and Autonomous Systems*, vol. 79, pp. 122-131, 2016.

[6] P Chen, J Xiang, W Wei. “A unified weighted least norm method for redundant manipulator control,” *International Journal of Advanced Robotic Syst*ems, vol. 13, no. 19, 2015.

[7] Nima Ramezani Taghiabadi, “Inverse Kinematics, Kinematic Control and Redundancy Resolution for Chained-Link Robotic Manipulators”, Faculty of Information Technology University of Technology, 2016.

[8] P Beeson, B Ames. “TRAC-IK: An open-source library for improved solving of generic inverse kinematics,” *IEEE-RAS International Conference on Humanoid Robots*, vol. 12, no. 12, pp. 928-935. December 2015.

[9] Meiling W, Minzhou L, Tao L, “A Unified Dynamic Control Method for a Redundant Dual Arm Robot,” *Journal of Bionic Engineering*, vol. 12, no. 3, pp.361-371, July 2015.

[10] R Diankov, P Rybski, “Automated Construction of Robotic Manipulation Programs.” Carnegie Mellon University, 2010.

[11] D Rakita, B Mutlu, M Gleicher. “RelaxedIK: Real-time Synthesis of Accurate and Feasible Robot Arm Motion,” Pittsburgh, PA, USA: *Robotics: Science and Systems*, vol. 10, June 2018.

[12] B Cohen, S Chitta, M Likhachev, “Single- and dual-arm motion planning with heuristic search,” *International Journal of Robotics Research*, vol. 12, no.7363472, pp. 928-935, December 2015.

[13] SungYul S, ChangHwan K, “Human-Like Motion Generation and Control for Humanoid’s Dual Arm Object Manipulation,” *IEEE Transmotions on Industrial Electronics*, vol. 62, no. 4, pp. 2265-2276, April 2015.

[14] Hongcheng X, Xilun D, “A Synergic Method for Anthropomorphic Dual-Arm Robots to Plan Bimanual Transport Tasks, ” Macau, China: *IEEE International Conference on Robotics and Biomimetics(ROBIO)*, vol. 2, no.1, pp. 1-6, January 2018.

[15] Shimizu M , Kakuya H , Yoon W K , et al, “Analytical Inverse Kinematic Computation for 7-DOF Redundant Manipulators With Joint Limits and Its Application to Redundancy Resolution,” *IEEE Transmotions on Robotics*, vol. 24, nol. 5, pp. 1131-1142, 2008.

[16] Sucan I A, Moll M, Kavraki L E. “The Open Motion Planning Library,” IEEE Robotics & Automation Magazine, vol. 19, nol.4, pp.72-82, 2012.

[17] K Kretuz-delgado, M Long, H Seraji. “Kinematic analysis of 7-DOF manipulators,” *The International journal of robotics research*, vol. 11, no. 5, pp. 469-481, October 1992.

[18] Pham, Quang-Cuong, “A General, Fast, and Robust Implementation of the Time-Optimal Path Parameterization Algorithm,” vol. 30, no. 6, pp 1533-1540, December 2014.